Available online at www.sciencedirect.com

ScienceDirect

Procedia Structural Integrity 24 (2019) 764–774

Structural Integrity Procedia

www.elsevier.com/locate/procedia

AIAS 2019 International Conference on Stress Analysis

Bending fatigue behaviour of 17-4 PH gears produced via selective laser melting

Luca Bonaiti[a,*], Franco Concli[b], Carlo Gorla[a], Francesco Rosa[a]

[a] *Department of Mechanical Engineering, Politecnico di Milano, via La Masa 1, 20157 Milano, Italy*
[b] *Faculty of Science and Technology, Free University of Bozen-Bolzano, piazza Università, 1, 39100 Bolzano, Italy*

Abstract

The possibility of producing parts via the addition of material, instead of its removing, given by Additive Manufacturing (AM) processes is changing the way in which parts are designed. However, the design of some mechanical components like gears, for instance, requires specific resistance data that, up to now, are not presented in literature. This paper presents a research project aimed at investigating the bending fatigue properties of 17-4 PH steel applied to gears produced via selective laser melting. Single Tooth bending Fatigue (STF) tests were conducted in order to investigate the S-N curve. Results are presented in terms of tooth root stress calculated according to the ISO standard in order to compare them with data of other materials. In addition, Scanning Electron Microscopy (SEM) of the fractured surfaces has been performed on the failed teeth to investigate failure origin and therefore to find causes of tooth breakage.

Keywords: 174-PH; selective laser melting; gears; bending fatigue; gearbox design

Nomenclature

b	Facewidth
d_{en}	diameter of the outer point of single pair tooth contact
F_t	Tangential force
h^*_{aP}	Addendum coefficient of the basic rack profile
h_{Fe}	Bending moment arm
h^*_{fP}	Dedendum coefficient of the basic rack profile
m_n	Normal module
q_S	Notch parameter

* Corresponding author. Tel.: +39 02-2399-8290; fax: +39-02-2399-8263.
E-mail address: luca.bonaiti@polimi.it

10.1016/j.prostr.2020.02.068

x	Profile shift coefficient
S_{Fn}	Tooth root chord
Y_B	Gear rim factor
Y_{DT}	Deep tooth factor
Y_F	Tooth form factor
Y_{NT}	life factor
Y_S	Stress correction factor
Y_β	Helix angle factor
z	Number of teeth
α_n	Normal Pressure angle
β	Pressure angle at normal section
ρ^*_{fP}	Root fillet radius coefficient of the basic rack profile
σ_{F0}	Tooth root stress
σ_{FP}	Permissible tooth root stress

Acronyms

AM Additive Manufacturing

ADI Austenite Ductile Iron

STF Single Tooth bending Fatigue

SEM Scanning Electron Microscope

SLM Selective Laser Melting

1. Introduction

Since its introduction in the commercial field, Additive Manufacturing (AM) has been showing an important growth. In the late '80s, AM has been introduced in the market for the production of models and prototypes, while nowadays it is used for the production of components that may also work in the real field (Thompson et al. (2016)). Also, it has also been proved that, for small quantities, production with AM is more cost-effective rather than producing parts with traditional technologies (f.i. see Atzeni and Salmi (2012)). Within this scenario, the production of gears with AM is a challenging topic; but few studies are present in literature in any case (f.i. see Kluge et al. (2017)).

As the design of a gear transmission must pass through standardized analytical methods, designers must be sure of the mechanical properties of the gear material. However, experience demonstrates that data coming directly from tested gears, not from simple standard specimens, have to be used to design this type of components. In the case of common materials (f.i. case hardened steel, cast iron, etc.), designers can rely on data already present within standard codes such as ISO 6336-5, 2006. However, due to the involved technology modernity, data related to gear produced via AM are not present in the aforementioned standards.

In this contest, we present a preliminary characterization of the tooth root bending behaviour for gears made by 17-4 PH and produced by Selective Laser Melting (SLM). In order to do that, we perform a Single Tooth bending Fatigue (STF) campaign aimed to determine the S-N curve. In addition, we present also the Scanning Electron Microscope (SEM) analysis of the failed teeth in order to understand the failure mode.

2. Test procedure

STF tests have been performed on a Schenk mechanical pulsator, whose scheme is shown in Fig. 1, capable to apply a maximum force of 60 kN. The methodology used for this experimental campaigns has already been applied

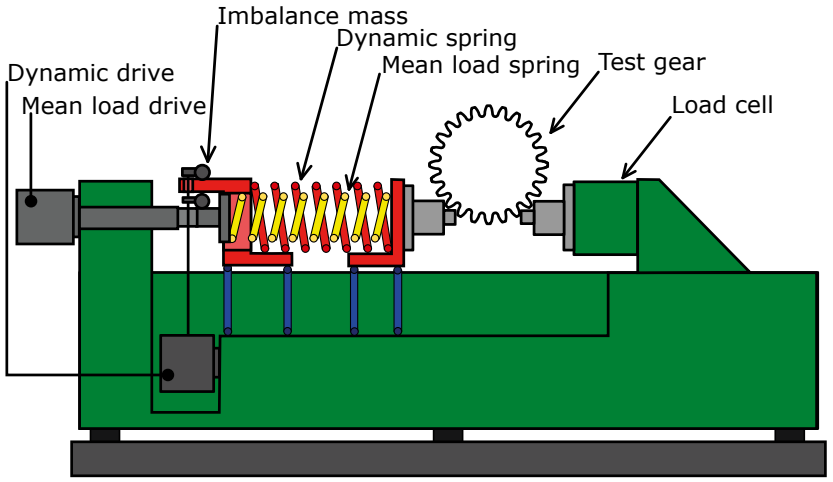

Fig. 1: Mechanical pulsator scheme.

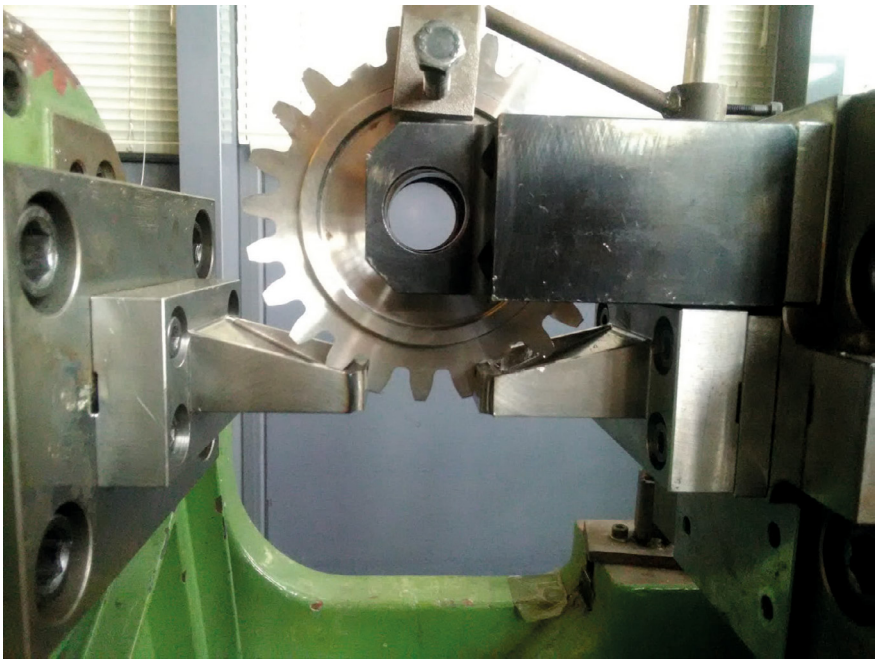

Fig. 2: Gear under testing.

by the authors to investigate the fatigue strength of other type of gears (f.i. see Gasparini et al. (2008), Gorla et al. (2012) and Gorla et al. (2017)). As in previous experimental campaigns, the equipment has been designed in order to have the contact between anvils and gear at a certain diameter, defined in a way such as it is possible to obtain a proper value of tooth root stress with respect to the range of loads that can be applied by the machine. As shown in Fig. 2 and Fig. 3, during our tests, the gear is positioned symmetrically between two anvils, and two teeth are loaded at the same height, resulting in a symmetric stress field at the tooth root.

In order to grant the symmetric positioning of the gear between the anvils, a pin and a fork are used. However, the resulting kinematic chain with pin, fork and anvils is statically indeterminate and it could affect the stress on the teeth. Therefore, before starting the tests, the pin is removed, ensuring the statically determinacy of the system.

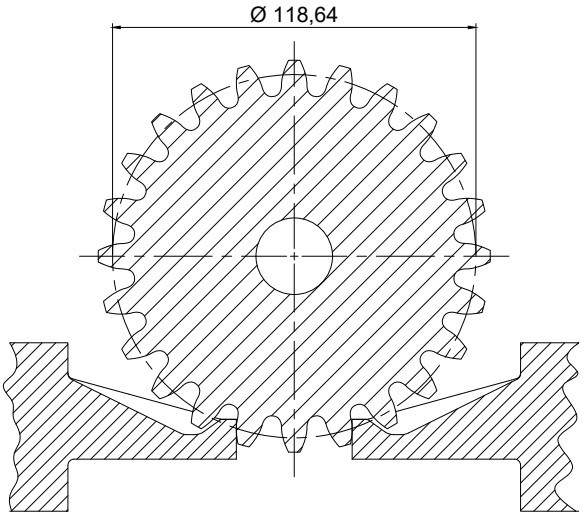

Fig. 3: Scheme of the gear/anvils contact.

As the pin has been removed, a minimum amount of compressive load has to be always present in order to keep the gear in the rightful position. Therefore, the test load is characterized with a load ratio R equal to 0.1. On the basis of authors' experience , this value is sufficient to ensure that undesired displacements will not take place during the test.

The test procedure is based on the following steps:

1. The gear is positioned by means of a pin and a fork opportunely designed.
2. A spring is connected to the gear to guarantee the quick removal of the gear after tooth failure.
3. The movable anvil is placed in contact with the teeth and a minimum pre-load is applied.
4. The pin is removed. The pre-load keeps the gear in position despite the vertical force applied by the spring.
5. Mean load is increased up to the test average value and then the oscillatory part is applied with an increasing amplitude, till it reaches the desired value.
6. When one of the two tested teeth breaks, the gear is removed by the spring and the machine stops automatically.

Tab. 1 and Fig.4 summarize all the gear dimensions, while Tab. 3 is the experimental matrix. The gears have been printed (Tab. 2 shows the main process parameters) and then machined with standard machine tools (i.e. lathe and hobbing machine). Material has been tested as-built without being subject to any thermal treatment.

3. Tooth root stress

Within Fig.5, we summarize the experimental results listed in Tab.3. The stress-load relation has been obtained by applying the procedure of ISO 6336-3 (2006) method B and considering only the relevant factors. According to the standard, we can write the tooth root stress as:

$$\sigma_{F0} = \frac{F_t}{bm_n} Y_F Y_s Y_\beta Y_B Y_{DT} \tag{1}$$

Table 1: STF gear main data.

Symbol	Value	Description
m_n	5 mm	Normal module
α_n	20°	Normal Pressure angle
β	0°	Pressure angle at normal section
z	24	Number of teeth
b	10 mm	Facewidth
x	0.2	Profile shift coefficient
h^*_{fP}	1.250	Dedendum coefficient of the basic rack profile
ρ^*_{fP}	0.380	Root radius factor of the basic rack profile
h^*_{aP}	1.00	Addendum coefficient of the basic rack profile

Table 2: Process parameter

Machine	EOS M280
Laser source	fiber
Printing direction	according to gear axis (see Fig. 4)
Gas	nitrogen
Power	200 W
Scanning speed	600 mm s^{-1}
Spot diameter	100 µm
Layer thickness	40 µm
Average particle size	42.61 µm

Table 3: Bending fatigue test results.

Test ID	Gear	Tested teeth	F_{min} N	F_{max} N	Cycles	Broken tooth
000001	A	1-3	-15000	-1500	202550	1
000002	A	5-7	-14000	-1400	229575	7
000003	A	9-11	-13000	-1300	3581879	11
000004	A	13-15	-12500	-1250	481897	13
000005	A	17-19	-12250	-1225	581951	17
000006	A	21-23	-11000	-1100	631460	21

where Y_β, Y_B and Y_{DT} have unitary value.

Y_F and Y_S have a not unitary value and they are calculated as in Eq.(2) and Eq.(3).

$$Y_F = \frac{\frac{6h_{Fe}}{m_n} cos(\alpha_{Fen})}{\left(\frac{s_{Fn}}{m_n}\right) cos(\alpha_n)} \tag{2}$$

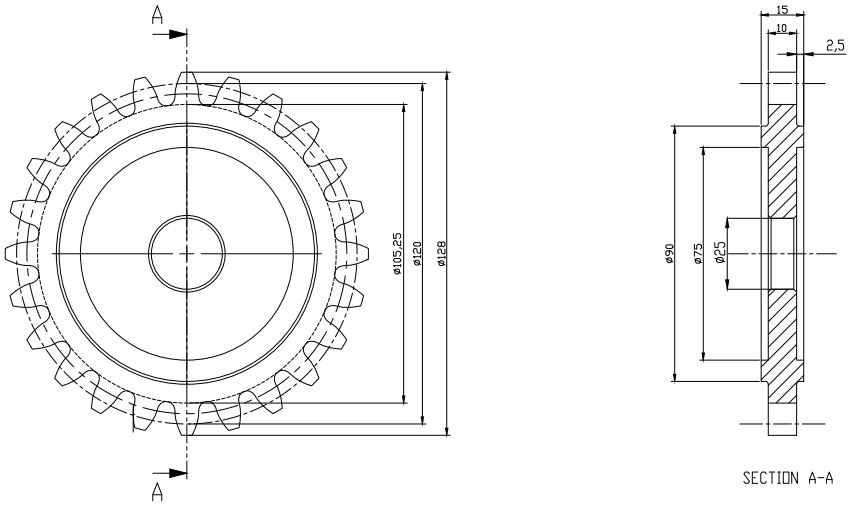

Fig. 4: Gear drawing.

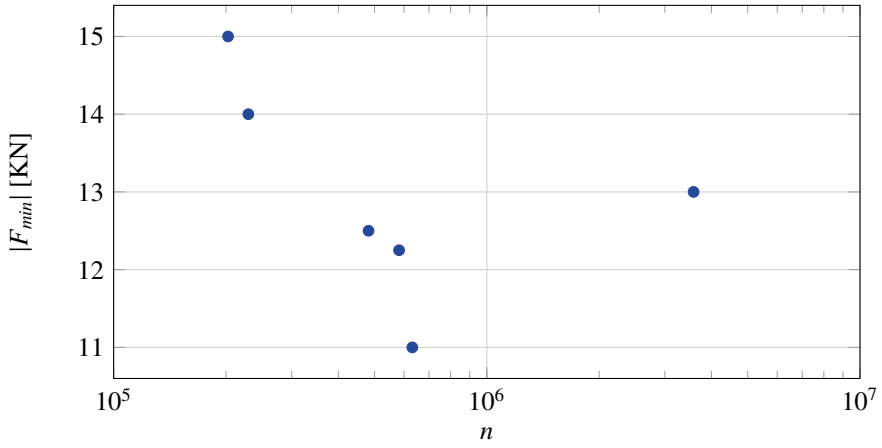

Fig. 5: Experimental points.

$$Y_S = (1.2 + 0.1L)q_s^{\frac{s_{Fn}}{1.2 + 2.3L}} \tag{3}$$

s_{Fn}, q_s and L are related only to the gear geometry and therefore they can be easily calculated with the equations included in ISO 6336-3 (2006). Some considerations have to be done regarding h_{Fe} and α_{Fen} because they are related to the outer point of single contact but, as we are dealing with STF test, we do not have two gears in contact. In the ISO 6336-3 (2006) standard, which suppose two meshed gears, h_{Fe} and α_{Fen} depend on d_{en}; that is the diameter of the outer point of single pair tooth contact. In our case, h_{Fe} and α_{Fen} and, subsequently, Y_F and Y_S, have been calculated with reference to the diameter where the load is applied.

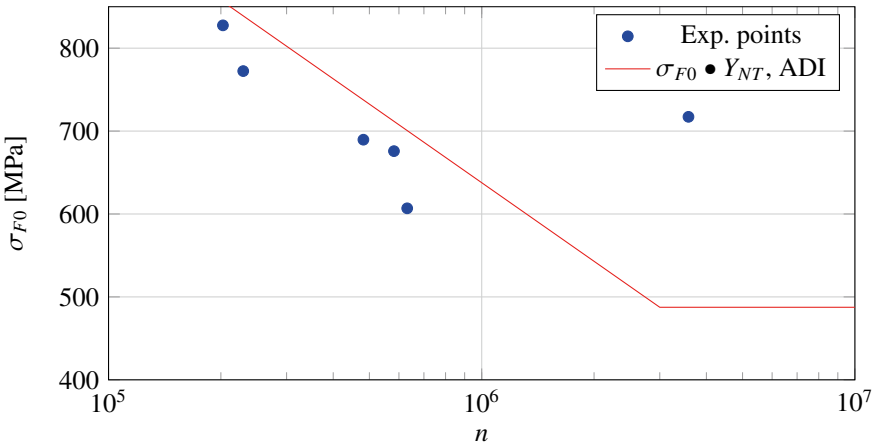

Fig. 6: S-N curve.

Table 4: Chemical analys of tooth A7 (Fig.8).

Position	% Si	% Cr	% Fe	%Ni	%Cu
A	0.69	17.36	73.74	4.59	3.61
B	1.13	28.37	67.29	2.33	0.88
C	0.93	17.09	74.83	3.94	3.20

According to the geometrical data shown in Tab.1 and to the gear/anvils contact scheme shown in Fig. 3, Y_F and Y_S result equal to 1.58 and 1.74 respectively. Therefore, Eq.(1) can be rewritten as:

$$\sigma_{F0} = 0.055 * F_t \tag{4}$$

where F_t is in N and σ_{F0} is in MPa.

By applying the above equation to the experimental data, we can elaborate the experimental points of Fig.5 in order to draw the S-N curve, shown in Fig. 6.

ISO 6336-5 (2006) presents fatigue limits for steel which are much higher than the tooth root stress data shown in the aforementioned figure: f.i., the bending fatigue limit for a case hardened wrought steel (Eh, ML quality) is about 600 MPa. Consequently, in order to compare the present experimental points whit the resistance of material used for common applications, Fig. 6 shows also the fatigue limit obtained by the authors from gears made in Austenite Ductile Iron (ADI) and with a similar geometry (see Gorla et al. (2018)); Y_{NT} has been taken from ISO 6336-3 (2006) considering the proper material type (nodular cats iron). It can been easily seen that the AM gears tested in this campaign have comparable fatigue properties.

4. SEM analysis

The last step of this preliminary experimental campaign has been the SEM analysis of the teeth fracture surface. In order to do that, all the failed teeth have been brittle broken in liquid nitrogen; Fig. 7 - 12 show the analysis results. By looking at those pictures, we can say that, for all the specimens, the fracture seems to originate from a single point and beach marks have not been observed.

The analysis highlights the presence of defects with considerable dimensions (see Fig. 7, Fig. 8, Fig. 9 and Fig. 10). Those shown in Fig. 9, Fig. 10 are the so-called "lack of fusion" defects. The punctual chemical analysis of tooth A7

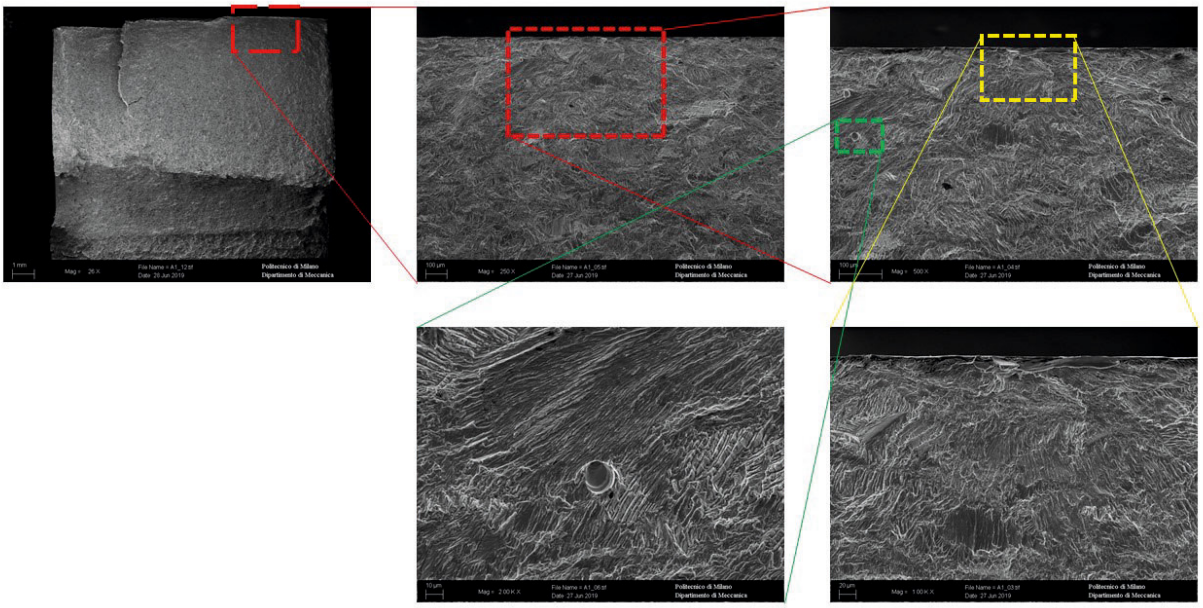

Fig. 7: SEM analysis of tooth A1, failed after 202550 cycles at 15 kN

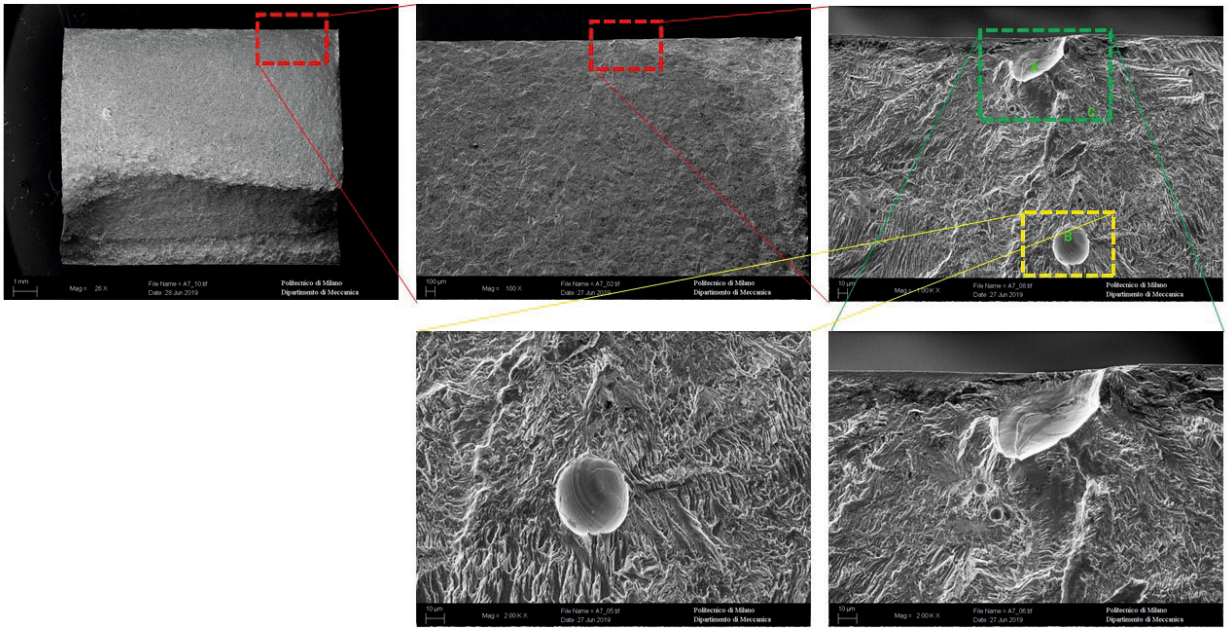

Fig. 8: SEM analysis of tooth A7, failed after 229575 cycles at 14 kN

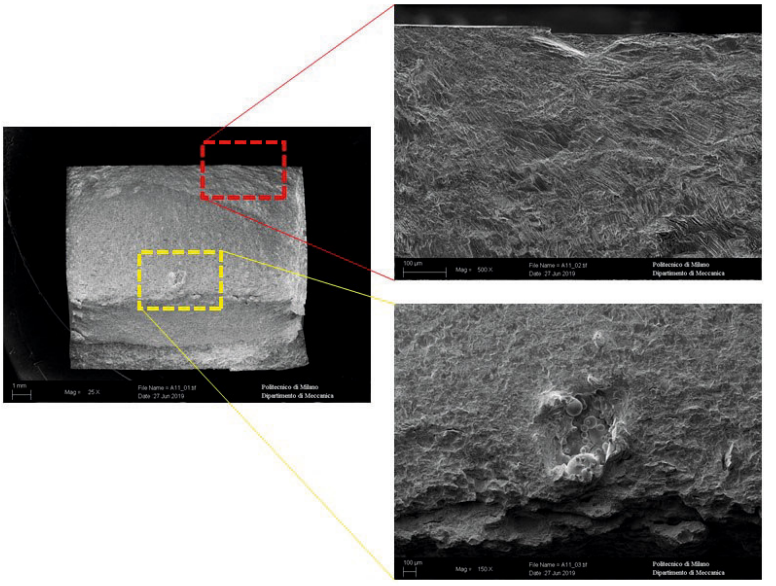

Fig. 9: SEM analysis of tooth A11, failed after 3581879 cycles at 13kN

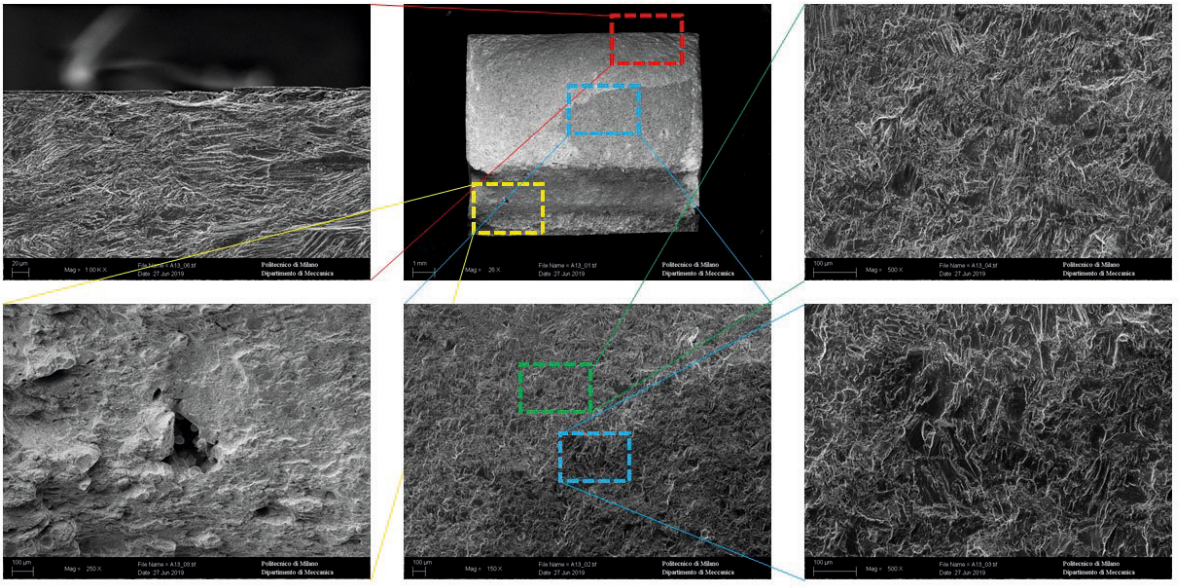

Fig. 10: SEM analysis of tooth A13, failed after 481897 cycles at 12.5kN

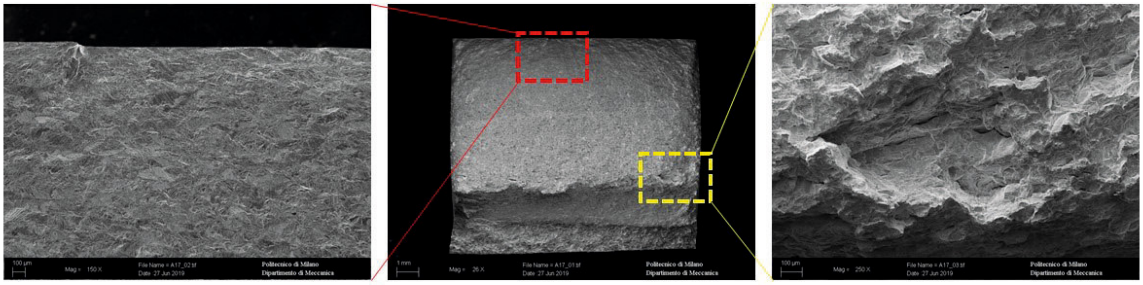

Fig. 11: SEM analysis of tooth A17, failed after 581951 cycles at 12.25kN

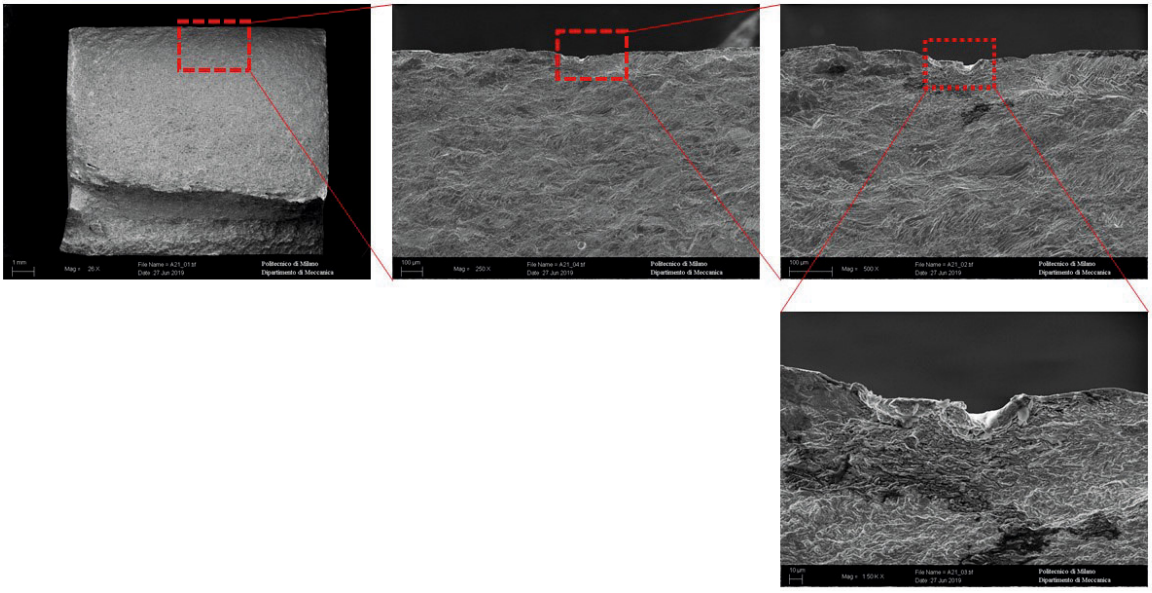

Fig. 12: SEM analysis of tooth A21, failed after 611460 cycles at 11kN

defects (reported in Tab. 4) did not show relevant differences with the base material; therefore, also those defects are catalogable as a lack of fusion. Furthermore, considering their proximity to the external surface, we can state that they are responsible of the failure. Also the spherical defect shown in Fig. 7 can be catalogued as a lack of fusion.

Yadollahi and Shamsaei (2017), Koutiri et al. (2018) and Mower and Long (2016) have studied the fatigue behaviour of parts produced via AM. Even if their work is focused on different materials, all the authors report that the presence of defects, typically "lack of fusions", has an important influence on the fatigue behaviour of AM components. The above considerations are in agreement with the result of the present campaign.

5. Conclusion

A preliminary STF experimental campaign aimed to characterize gears made by 17-4 PH produced via SLM has been performed. In this way, it has been possible to obtain an initial characterization of tooth root bending fatigue obtained directly from gears.

By comparing the experimental results with data found in literature, it can be noticed that the properties of AM gears are lower than those of gears made by standard steel; however, their properties seems to be comparable to the ones of ADI gears. This behaviour can be explained on the basis of the performed SEM analysis, which highlight an important presence of defects within the material (mainly lack of fusion). Those defects, as found in literature, affects the AM gear performances.

Due to the limited amount of experimental data, this preliminary conclusions have to be confirmed by additional test and the experimental campaign is still on-going.

Funding

The authors would like to thank the Free University of Bozen-Bolzano for the financial support given to this study through the project M.AM.De (TN2092, call CRC2017 Unibz PI Franco Concli franco.concli@unibz.it).

References

Atzeni, E., Salmi, A., 2012. Economics of additive manufacturing for end-usable metal parts. The International Journal of Advanced Manufacturing Technology 62, 1147–1155.

Gasparini, G., Mariani, U., Gorla, C., Filippini, M., Rosa, F., 2008. Bending fatigue tests of helicopter case carburized gears: Influence of material, design and manufacturing parameters, in: American Gear Manufacturers Association (AGMA) Fall Technical Meeting, pp. 131–142.

Gorla, C., Conrado, E., Rosa, F., Concli, F., 2018. Contact and bending fatigue behaviour of austempered ductile iron gears. Proceedings of the Institution of Mechanical Engineers, Part C: Journal of Mechanical Engineering Science 232, 998–1008.

Gorla, C., Rosa, F., Concli, F., Albertini, H., 2012. Bending fatigue strength of innovative gear materials for wind turbines gearboxes: Effect of surface coatings, in: ASME 2012 International Mechanical Engineering Congress and Exposition, American Society of Mechanical Engineers. pp. 3141–3147.

Gorla, C., Rosa, F., Conrado, E., Concli, F., 2017. Bending fatigue strength of case carburized and nitrided gear steels for aeronautical applications. International Journal of Applied Engineering Research 12, 11306–11322.

ISO 6336-3, 2006. Calculation of load capacity of spur and helical gears, part 3: Calculation of tooth bending strength. International Standard Organization, Geneva .

ISO 6336-5, 2006. Calculation of load capacity of spur and helical gears, part 5: Strength and quality of materials. International Standard Organization, Geneva .

Kluge, M., Kotthoff, G., Cavallini, C., Driveline, G., Höges, S., Metallurgy, G.P., 2017. Design and production of innovative transmission components with additive manufacturing, in: Proceedings from 16th International CTI Symposium Automotive Transmissions, HEV and EV Drives.

Koutiri, I., Pessard, E., Peyre, P., Amlou, O., De Terris, T., 2018. Influence of slm process parameters on the surface finish, porosity rate and fatigue behavior of as-built inconel 625 parts. Journal of Materials Processing Technology 255, 536–546.

Mower, T.M., Long, M.J., 2016. Mechanical behavior of additive manufactured, powder-bed laser-fused materials. Materials Science and Engineering: A 651, 198–213.

Thompson, M.K., Moroni, G., Vaneker, T., Fadel, G., Campbell, R.I., Gibson, I., Bernard, A., Schulz, J., Graf, P., Ahuja, B., et al., 2016. Design for additive manufacturing: Trends, opportunities, considerations, and constraints. CIRP annals 65, 737–760.

Yadollahi, A., Shamsaei, N., 2017. Additive manufacturing of fatigue resistant materials: Challenges and opportunities. International Journal of Fatigue 98, 14–31.